A Configuration Interaction approach to hole pairing in the Two-Dimensional Hubbard Model

E. Louis
Departamento de Física Aplicada, Universidad de Alicante, Apartado 99, E-03080 Alicante, Spain.

F. Guinea, M. P. López Sancho, J. A. Vergés
Instituto de Ciencia de Materiales de Madrid, CSIC, Cantoblanco, E-28049 Madrid, Spain.
(February 1, 2008)

The interactions between holes in the Hubbard model, in the low density, intermediate to strong coupling limit, are investigated by systematically improving mean field calculations. The Configuration Interaction basis set is constructed by applying to local Unrestricted Hartree-Fock configurations all lattice translations and rotations. It is shown that this technique reproduces, correctly, the properties of the Heisenberg model, in the limit of large U. Upon doping, dressed spin polarons in neighboring sites have an increased kinetic energy and an enhanced hopping rate. Both effects are of the order of the hopping integral and lead to an effective attraction at intermediate couplings. The numerical results also show that when more than two holes are added to the system, they do not tend to cluster, but rather hole pairs remain far appart. Hole–hole correlations are also calculated and shown to be in qualitative agreement with exact calculations for 4×4 clusters. In particular our results indicate that for intermediate coupling the hole–hole correlation attains a maximum when the holes are in the same sublattice at a distance of $\sqrt{2}$ times the lattice spacing, in agreement with exact results and the t–J model. The method is also used to derive known properties of the quasiparticle band structure of isolated spin polarons.

PACS number(s): 74.20.-z, 02.70.Lq, 71.10.Fd

I. INTRODUCTION

The nature of the low energy excitations in the Hubbard model has attracted a great deal of attention. It is well established that At half–filling the ground state is an antiferromagnetic (AF) insulator. Also, there exists conclusive evidence which indicates that antiferromagnetism is rapidly suppressed upon doping [1,2]. Close to half filling, a large amount of work suggests the existence of spin polarons, made of dressed holes, which propagate within a given sublattice with kinetic energy which in the strong coupling limit is of the order of $J = \frac{4t^2}{U}$ [3,4], where t is the hopping integral and U the on site Coulomb repulsion. These results are consistent with similar calculations in the strong coupling, low doping limit of the Hubbard model, the $t - J$ model [5–7]. There is also evidence for an effective attraction between these spin polarons [8–10,37,12,13]. However, recent and extensive Monte Carlo calculations for 0.85 filling and $U = 2 - 8t$, have shown that the pairing correlations vanish as the system size or the interaction strength increases [14].

We have recently analyzed the dynamics of spin polarons [15,16] and the interactions between them [17] by means of a systematic expansion around mean field calculations of the Hubbard model. Two spin polarons in neighboring sites experience an increase in their internal kinetic energy, due to the overlap of the charge cloud. This repulsion is of the order of t. In addition, a polaron reduces the obstacles for the diffusion of another, leading to an assisted hopping term which is also of same order. The combination of these effects is an attractive interaction at intermediate values of U/t. The purpose of this work is to discuss in detail the results and the approach proposed in [17]. We present new results which support the validity of our approach, highlighting the physically appealing picture of pairing that it provides. An alternative scheme to go beyond the unrestricted Hartree Fock approximation is to supplement it with the Gutzwiller projection method, or, equivalently, slave boson techniques [18,19]. These results are in agreement with the existence of significant effects due to the delocalization of the solutions, as reported here.

The rest of the paper is organized as follows. In Section II we discuss the physical basis of our proposal and the way in which we implement the Configuration Interaction method. A discussion of the limit of large U/t in the undoped case is presented in Section III. It is shown that, contrary to some expectations, the Hartree-Fock scheme reproduces correctly the mean field solution of the Heisenberg model. The systematic corrections analyzed here can be put in precise correspondence with similar terms discussed for quantum antiferromagnets. Results for the 4×4 cluster are compared with exact results in Section IV. Section V is devoted to discuss our results for a single hole (spin polaron)

and for two or more holes. The hole–hole correlations are also presented in this Section. The last Section is devoted to the conclusions of our work.

II. METHODS

A. Hamiltonian

We investigate the simplest version of the Hubbard Hamiltonian used to describe the dynamics of electrons in CuO_2 layers, namely,

$$H = T + C \ , \tag{1a}$$

$$T = \sum_{\sigma} T^{\sigma} = -\sum_{\langle ij \rangle} t_{ij} c^{\dagger}_{i\sigma} c_{j\sigma} \ , \tag{1b}$$

$$C = \sum_{i} U_i n_{i\uparrow} n_{i\downarrow} \ . \tag{1c}$$

The Hamiltonian includes a single atomic orbital per lattice site with energy E_i=0. The sums are over all lattice sites $i = 1, N_s$ of the chosen cluster of the square lattice and/or the z component of the spin ($\sigma = \uparrow, \downarrow$). The operator $c_{j\sigma}$ destroys an electron of spin σ at site i, and $n_{i\sigma} = c^{\dagger}_{i\sigma} c_{i\sigma}$ is the local density operator. t_{ij} is the hopping matrix element between sites i and j (the symbol $\langle ij \rangle$ denotes that the sum is restricted to all nearest neighbors pairs) and U_i is the intrasite Coulomb repulsion. Here we take $t_{ij} = t$ and $U_i = U$, and the lattice constant as the unit of length.

B. Unrestricted Hartree–Fock (UHF) solutions

As we shall only consider UHF solutions having a local magnetization pointing in the same direction everywhere in the cluster, we shall use the most simple version of the UHF approximation [20]. Within this approximation the effective mean field Hamiltonian that accounts for the Hubbard term is written as,

$$C^{\rm eff} = \sum_{\sigma} X^{\sigma} - U \sum_{i} \langle n_{i\uparrow} \rangle \langle n_{i\downarrow} \rangle \ , \tag{2a}$$

$$X^{\sigma} = U \sum_{i} n_{i\sigma} \langle n_{i\sigma} \rangle \ . \tag{2b}$$

The full UHF Hamiltonian is then written as,

$$H^{\rm UHF} = T + C^{\rm eff} \ . \tag{3}$$

Use of the Unrestricted Hartree Fock (UHF) approximation in finite clusters provides a first order approximation to the spin polaron near half filling. As discussed elsewhere, the UHF approximation describes well the undoped, insulating state at half filling [20] (see also next Section). A realistic picture of the spin wave excitations is obtained by adding harmonic fluctuations by means of the time dependent Hartree Fock approximation (RPA) [21]. At intermediate and large values of U/t, the most stable HF solution with a single hole is a spin polaron [20,15]. In this solution, approximately half of the charge of the hole is located at a given site. The spin at that site is small and it is reversed with respect to the antiferromagnetic background. The remaining charge is concentrated in the four neighboring sites. A number of alternative derivations lead to a similar picture of this small spin bag [22–25]. A similar solution is expected to exist in the $t - J$ model.

A schematic picture of the initial one hole and two holes Hartree Fock wavefunctions used in this work is shown in Fig. 1. They represent the solutions observed at large values of U/t for the isolated polaron and two spin polarons on neighboring sites. The electronic spectrum of these configurations show localized states which split from the top of the valence band.

As usual in mean field theories, the UHF solutions for an arbitrary number of holes [20], such as the spin polaron solution described above, break symmetries which must be restored by quantum fluctuations. In particular, it breaks spin symmetry and translational invariance (see Fig. 1). Spin isotropy must exist in finite clusters. However, it is spontaneously broken in the thermodynamic limit, due to the presence of the antiferromagnetic background. Hence, we do not expect that the lack of spin invariance is a serious drawback of the Hartree Fock solutions (this point is analyzed, in some detail in [21]). Results obtained for small clusters [16,26] show a slight improvement of the energy, which goes to zero as the cluster size is increased. On the other hand, translational invariance is expected to be present in the exact solution of clusters of any size. The way we restore translational invariance is discussed in the following subsection. Finally we know how to estimate the effects due to zero point fluctuations around the UHF ground state [21]. For spin polarons these corrections do not change appreciably the results, although they are necessary to describe the long range magnon cloud around the spin polaron [27].

C. Configurations Interaction (CI) method

We have improved the mean field results by following the procedure suggested years ago by some of us [15]. We hybridize a given spin UHF solution with all wavefunctions obtained from it by lattice translations. In the case of two or more holes point symmetry has also to be restored. This is accomplished by applying rotations to the chosen configuration. Configurations generated from a given one through this procedure are degenerate in energy and interact strongly. Here we have also investigated the effect of extending the basis by including other configurations having different energies. In all cases we include sets of wavefunctions with the lattice symmetry restored as mentioned.

In a path integral formulation, this procedure would be equivalent to calculating the contribution from instantons which visit different minima. On the other hand, it is equivalent to the Configuration Interaction (CI) method used in quantum chemistry. The CI wavefunction for a solution corresponding to N_e electrons is then written as

$$\Psi(N_e) = \sum_i a_i \Phi^i(N_e) \ , \tag{4}$$

where the set $\Phi^i(N_e)$ is formed by some chosen UHF wavefunctions (Slater determinants) plus those obtained from them by all lattice translations and rotations. The coefficients a_i are obtained through diagonalization of the exact Hamiltonian. The same method, using homogeneous paramagnetic solutions as starting point, has been used in [28].

The wavefunctions forming this basis set are not in principle orthogonal. Thus, both wavefunctions overlap and non–diagonal matrix elements of the Hamiltonian need to be taken into account when mixing between configurations is considered.

If only configurations having the same energy and corresponding, thus, to the same UHF Hamiltonian, are included, a physically sound decomposition of the exact Hamiltonian is the following [16],

$$H = H^{\rm UHF} + C - \sum_\sigma X^\sigma + U \sum_i \langle n_{i\uparrow}\rangle\langle n_{i\downarrow}\rangle \ , \tag{5}$$

In writing the matrix elements of this Hamiltonian we should note that the basis formed by the wavefunctions Φ_i is not orthogonal. Then, we obtain,

$$H_{ij} = \left(E^{\rm UHF} + U \sum_i \langle n_{i\uparrow}\rangle\langle n_{i\downarrow}\rangle \right) S_{ij} + C_{ij} - \sum_\sigma X^\sigma_{ij} S^{\bar\sigma}_{ij} \tag{6}$$

where $E^{\rm UHF}$ is the UHF energy of a given mean field solution, and the matrix elements of the overlap S are given by

$$S_{ij} = \langle \Phi^i(N_e) | \Phi^j(N_e)\rangle = S^\uparrow_{ij} S^\downarrow_{ij} \tag{7}$$

This factorization is a consequence of the characteristics of the mean field solutions considered in this work (only one component of the spin different from zero). The specific expression for the matrix elements of the overlap is,

$$S^\sigma_{ij} = \begin{vmatrix} < \phi^{i\sigma}_1 | \phi^{j\sigma}_1 > & ... & < \phi^{i\sigma}_1 | \phi^{j\sigma}_{N_\sigma} > \\ ... & ... & ... \\ < \phi^{i\sigma}_{N_\sigma} | \phi^{j\sigma}_1 > & ... & < \phi^{i\sigma}_{N_\sigma} | \phi^{j\sigma}_{N_\sigma} > \end{vmatrix} \tag{8}$$

where the number of particles for each component of the spin are determined from the usual conditions, $N_\uparrow + N_\downarrow = N_e$ and $N_\uparrow - N_\downarrow = 2S_z$. The $\phi^{i\sigma}_n$ are the monoelectronic wavefunctions corresponding to the Slater determinant i,

$$|\phi_n^{i\sigma}\rangle = \sum_k \alpha_{nk}^{i\sigma} c_{k\sigma}^\dagger |0\rangle, \tag{9}$$

$\alpha_{nk}^{i\sigma}$ being real coefficients obtained through diagonalization of the $H^{\rm UHF}$ Hamiltonian. The matrix element of the exchange operator between Slater determinants i and j is,

$$X_{ij}^\sigma = \begin{vmatrix} < \phi_1^{i\sigma}|X^\sigma\phi_1^{j\sigma} > & ... & < \phi_1^{i\sigma}|\phi_{N_\sigma}^{j\sigma} > \\ ... & ... & ... \\ < \phi_{N_\sigma}^{i\sigma}|X^\sigma\phi_1^{j\sigma} > & ... & < \phi_{N_\sigma}^{i\sigma}|\phi_{N_\sigma}^{j\sigma} > \end{vmatrix} + ... + \begin{vmatrix} < \phi_1^{i\sigma}|\phi_1^{j\sigma} > & ... & < \phi_1^{i\sigma}|X^\sigma\phi_{N_\sigma}^{j\sigma} > \\ ... & ... & ... \\ < \phi_{N_\sigma}^{i\sigma}|\phi_1^{j\sigma} > & ... & < \phi_{N_\sigma}^{i\sigma}|X^\sigma\phi_{N_\sigma}^{j\sigma} > \end{vmatrix} \tag{10}$$

where the matrix elements of X^σ between monoelectronic wavefunctions are given by,

$$< \phi_n^{i\sigma}|X^\sigma\phi_m^{j\sigma} >= U\sum_k \alpha_{nk}^{i\sigma}\alpha_{mk}^{j\sigma}\langle n_{k\bar\sigma}\rangle \tag{11}$$

On the other hand the matrix elements of C are,

$$C_{ij} = U\sum_k \left(n_{k\uparrow}\right)_{ij}\left(n_{k\downarrow}\right)_{ij} \tag{12}$$

where each $\left(n_{k\sigma}\right)_{ij}$ is given by an equation similar to Eq. (10). The matrix elements of the density operator between monoelectronic wavefunctions are,

$$< \phi_n^{i\sigma}|n_{k\sigma}\phi_m^{j\sigma} >= \alpha_{nk}^{i\sigma}\alpha_{mk}^{j\sigma} \tag{13}$$

If the CI basis includes wavefunctions having different UHF energies, the above procedure is not valid and one should calculate the matrix elements of the original exact Hamiltonian. Although this is in fact reduced to calculate the matrix elements of the kinetic energy operator T, the procedure is slightly more costly (in terms of computer time) than the one described above. The matrix elements of the exact Hamiltonian in the basis of Slater determinants are,

$$H_{ij} = \sum_\sigma T_{ij}^\sigma S_{ij}^{\bar\sigma} + C_{ij} \tag{14}$$

where T_{ij}^σ are given by an equation similar to Eq. (10), and the matrix elements of the kinetic energy operator between monoelectronic wavefunctions are

$$< \phi_n^{i\sigma}|T^\sigma\phi_m^{j\sigma}\rangle = -t\sum_{<kl>} \alpha_{nk}^{i\sigma}\alpha_{ml}^{j\sigma} \tag{15}$$

The matrix elements involved in the calculation of hole–hole correlations for a given CI wavefunction are similar to those that appeared in the computation of the Hubbard term. In particular the following expectation value has to be computed,

$$\langle\Psi|(1-n_k)(1-n_l)|\Psi\rangle = \sum_{ij} a_i a_j \langle\Phi_i|(1-n_k)(1-n_l)|\Phi_j\rangle \tag{16}$$

where $n_k = n_{k\uparrow} + n_{k\downarrow}$. Terms of four operators in this expectation value are similar to Eq. (12). Those requiring more computer time involve $n_{k\uparrow}n_{l\uparrow}$ with $k \neq l$,

$$\left(n_{k\uparrow}n_{l\uparrow}\right)_{ij} = \begin{vmatrix} < \phi_1^{i\sigma}|n_{k\uparrow}\phi_1^{j\sigma} > & < \phi_1^{i\sigma}|n_{l\uparrow}\phi_2^{j\sigma} > & ... & < \phi_1^{i\sigma}|\phi_{N_\sigma}^{j\sigma} > \\ ... & ... & ... & ... \\ < \phi_{N_\sigma}^{i\sigma}|n_{k\uparrow}\phi_1^{j\sigma} > & < \phi_{N_\sigma}^{i\sigma}|n_{l\uparrow}\phi_2^{j\sigma} > & ... & < \phi_{N_\sigma}^{i\sigma}|\phi_{N_\sigma}^{j\sigma} > \end{vmatrix} + \text{permutations} \tag{17}$$

D. Numerical Calculations

Calculations have been carried out on $L\times L$ clusters with periodic boundary conditions ($L \leq 12$) and $U = 8-5000t$. Some results for lower values of U are also presented. Note that $U = 8t$ is widely accepted as the most physically

meaningful value of Coulomb repulsion in these systems (see for instance [29]). Although larger clusters can be easily reached, no improvement of the results is achieved due to the short–range character of the interactions (see below).

The numerical procedure runs as follows. Localized UHF solutions are first obtained and the Slater determinants for a given filling constructed. The full CI basis set is obtained by applying all lattice traslations to the chosen localized UHF Slater determinants all having the same z component of the spin S_z. Then we calculate the matrix elements of the overlap and of the Hamiltonian in that basis set. This is by far the most time consuming part of the whole calculation. Diagonalization is carried out by means of standard subroutines for non–orthogonal bases. The state of lowest energy corresponds to the CI ground state of the system for a given S_z. The desired expectation values are calculated by means of this ground state wavefunction. The procedure is variational and, thus, successive enlargements of the basis set do always improve the description of the ground state.

III. THE LIMIT OF LARGE U IN THE UNDOPED CASE.

The Hartree Fock scheme, for the undoped Hubbard model in a square lattice gives an antiferromagnetic ground state, with a charge gap. At large values of U/t, the gap is of order U. The simplest correction beyond Hartree-Fock, the RPA approximation, leads to a continuum of spin waves at low energies [21]. Thus, the qualitative features of the solution are in good agreement with the expected properties of an antiferromagnetic insulator.

There is, however, a great deal of controversy regarding the adequacy of mean field techniques in describing a Mott insulator [30,31]. In principle, the Hubbard model, in the large U limit, should describe well such a system. At half filling and large U, the only low energy degrees of freedom of the Hubbard model are the localized spins, which interact antiferromagnetically, with coupling $J = \frac{4t^2}{U}$. It has been argued that, as long range magnetic order is not relevant for the existence of the Mott insulator, spin systems with a spin gap are the most generic realization of this phase. A spin gap is often associated with the formation of an RVB like state, which cannot be adiabatically connected to the Hartree Fock solution of the Hubbard model. So far, the best examples showing these features are two leg spin 1/2 ladders [33]. Recent work [34] indicates that, in the presence of magnetic order, the metal insulator transition is of the Slater type, that is, coherent quasiparticles can always be defined in the metallic side. These results seem to favor the scenario suggested in [30], and lend support to our mean field plus corrections approach.

Without entering into the full polemic outlined above, we now show that the method used here gives, in full detail, the results which can be obtained from the Heisenberg model by expanding around the antiferromagnetic mean field solution [34]. Such an expansion gives a consistent picture of the physics of the Heisenberg model in a square lattice.

The ground state energy of the Hartree Fock solution in a 4×4 cluster is compared to the exact value [8] at large values of U in Table I. The corresponding Heisenberg model is:

$$H_{\rm Heis} = \frac{4t^2}{U} \sum_{ij} \vec{\mathbf{S}}_i \vec{\mathbf{S}}_j - \frac{t^2}{U} \sum_{ij} n_i n_j \tag{18}$$

In a 4×4 cluster, the exact ground state energy is

$$E_{\rm Heis} = -16(c + 0.5)\frac{4t^2}{U} \tag{19}$$

where $c = 0.702$ [35], in good agreement with the results for the Hubbard model. The mean field energy can be parametrized in the same way, except that $c = 0.5$. This is the result that one expects for the mean field solution of the Heisenberg model, which is given by a staggered configuration of static spins. This solution can be viewed as the ground state of an anisotropic Heisenberg model with $J_z = J$ and $J_\pm = 0$.

We now analyze corrections to the Hartree Fock solution by hybridizing it with mean field wavefunctions obtained from it by flipping two neighboring spins (hereafter referred to as sf). These solutions are local extrema of the mean field solutions in the large U limit. In Table I we show the energy difference between these states and the antiferromagnetic (AF) Hartree Fock ground state, and their overlap and matrix element also with the ground state. We have checked that these are the only wavefunctions with a non negligible mixing with the ground state. The overlap goes rapidly to zero, and the energy difference and matrix elements adjust well to the expressions

$$\Delta E_{\rm AF,sf} = E_{\rm AF} - E_{\rm sf} = \frac{12t^2}{U} \tag{20a}$$

$$t_{\rm AF,sf} = \frac{2t^2}{U} \ . \tag{20b}$$

These are the results that one obtains when proceeding from the Heisenberg model. These values, inserted in a perturbative analysis of quantum corrections to the ground state energy of the Heisenberg model [34], lead to excellent agreement with exact results (see also below).

As already pointed out, in the CI calculation of the ground state energy we only include the mean field wavefunctions with two neighboring spins flipped. Restoring point symmetry gives a total of 4 configurations, while applying lattice translations leads to a set of $4L^2/2$ configurations (remember that configurations on different sublattices do not interact) to which the AF wavefunction has to be added. In the case of the 4×4 cluster the set has a total of 33 configurations. The CI energy for this cluster is given in Table I along with the exact and the UHF energies. It is noted that the CI calculation reduces in 50% the difference between the exact and the mean field result. Improving this results would require including a very large set, as other configurations do only decrease the ground state energy very slightly.

In the large U limit, the largest interaction is $t_{\rm AF,sf}$. Then, neglecting the overlap between the AF and the sf mean field solutions, the CI energy of the ground state can be approximated by,

$$E_{\rm CI} = \frac{1}{2}\left[E_{\rm AF} + E_{\rm sf} - \Delta E_{\rm AF,sf}\sqrt{1+\frac{8L^2t_{\rm AF,sf}^2}{(\Delta E_{\rm AF,sf})^2}}\right] \tag{21}$$

For $U = 50$ this expression gives $E_{\rm CI}$=-1.421, in excellent agreement with the CI result given in Table I.

Note that a perturbative calculation of the corrections of the ground state energy in finite clusters is somewhat tricky, as the matrix element scales with $\sqrt{N_s}$, where $N_s = L^2$ is the number of sites in the cluster, while the energy difference is independent of N_s. The first term in a perturbative expansion (pe) coincides with the first term in the expansion of the square root in Eq. (21),

$$E_{\rm pe} = E_{\rm AF} - \frac{2L^2t_{\rm AF,sf}^2}{\Delta E_{\rm AF,sf}} \tag{22}$$

in agreement with the result reported in [34]. Although this correction to the AF energy has the expected size dependence for an extensive magnitude (it is proportional to the number of sites N_s) and gives an energy already very similar to the exact, it was obtained by inconsistently expanding in terms of a parameter that can be quite large. For instance in the 4×4 cluster and U=50, $E_{\rm pe} \approx 1.51$, close to the exact result (Table I) while $(8L^2t_{\rm AF,sf}^2)/(\Delta E_{\rm AF,sf})^2 \approx 3.9$ much larger than 1. Thus, perturbation theory is doomed to fail even for rather small clusters.

On the other hand, the CI calculation described above introduce a correction to the AF energy which has not the correct size dependence. This can be easily checked in the large cluster limit in which the CI energy can be approximated by

$$E_{\rm CI} \approx \frac{1}{2}\left(E_{\rm AF} + E_{\rm sf}\right) - \sqrt{2}Lt_{\rm AF,sf} \tag{23}$$

while the correct expression should scale as N_s, because, in large clusters, the difference between the exact and the Hartree-Fock ground state energies must be proportional to N_s, irrespective of the adequacy of the Hartree-Fock approximation.

Thus, one obtains a better approximation to the ground state energy in the thermodynamic limit, by using the perturbative calculations in small clusters and extrapolating them to large clusters, as in the related $t-J$ model [34]. In any case, the problem outlined here does not appear when calculating corrections to localized spin textures, such as the one and two spin polarons analyzed in the next sections. The relevant properties are associated to the size of the texture, and do not scale with the size of the cluster they are embedded in.

From the previous analysis, we can safely conclude that our scheme gives a reliable approximation to the undoped Hubbard model in a square lattice in the strong coupling regime, $U/t \gg 1$. We cannot conclude whether the method is adequate or not for the study of models which exhibit a spin gap. It should be noted, however, that a spin gap needs not only be related to RVB like ground states. A spin system modelled by the non linear sigma model can also exhibit a gap in the ground state, if quantum fluctuations, due to dimensionality or frustration, are sufficiently large. In this case, a mean field approach plus leading quantum corrections should be qualitatively correct.

IV. COMPARISON WITH EXACT RESULTS FOR 4×4 CLUSTERS WITH TWO HOLES

In order to evaluate the performance of our approach we have calculated the ground state energy of two holes in the 4×4 cluster and compared the results with those obtained by means of the Lanczos method [8]. The results are

reported in Tables II–IV, where the energies for one hole are also given for the sake of completness (a full discussion of this case can be found in [15], see also below). In the case of one hole the standard spin polaron solution (Fig. 1) plus those derived from it through lattice translations form the basis set. For two holes we consider solutions with $S_z = 0$ or 1. In the first case we include either the configuration having the two holes at the shortest distance, i.e., separated by a (1,0) vector and/or at the largest distance possible, that is separated by a (2,1) vector, and those obtained from them through rotations. The basis used for the two polarons at the shortest distance is shown in Fig. 2. The set of these four configuration has the proper point symmetry. Again, lattice translations are applied to these configurations to produce the basis set with full translational symmetry. On the other hand, wavefunctions with $S_z = 1$ can be constructed by including configurations with the two holes separated by vectors (1,1) and/or (2,2).

The results for the energies of wavefunctions with $S_z = 0$ for several values of the interaction parameter U are reported in Tables II and III. As found for a single hole, the kinetic energy included by restoring the lattice symmetry, improves the wavefunction energies [15]. The improvement in the energy is larger for intermediate U. For instance for $U = 32$ a 10% gain is noted. Within UHF, the solution with the holes at the largest distance is more favorable for $U > 8t$. Instead, restoring the translational and point symmetries favors the solution with the holes at neighboring sites for all U shown in the Tables. The results also indicate that the correction introduced by this procedure does no vanish with U. A more detailed discussion of the physical basis of this result along with results for larger values of U and larger clusters will be presented in the following Section. On the other hand the energies get closer to the exact energies (see Table II). A further improvement in the energy is obtained by including both UHF configurations, namely, {1,0} and {2,1}. This improvement is larger for intermediate U and vanishes as U increases (Table III). Other configurations, such as that proposed in [40] in which the two holes lie on neighboring sites along a diagonal and a neighboring spin is flipped, may contribute to further improve the CI energy of the ground state.

It is interesting to compare these results with those corresponding to wavefunctions with $S_z = 1$ also reported in Table IV. It is noted that for $U = 6 - 16$ the energy of the solution including all configurations from the set {1,1} is smaller than those obtained with all configurations from either the set {1,0} or the set {2,1}. However, the wavefunction constructed with all configurations from the last two sets is more favorable than the best wavefunction with $S_z = 1$. The latter is in agreement with exact calculations [8] which obtained a ground state wavefunction with $S_z = 0$.

V. RESULTS

A. Single Polaron

Here we only consider the quasiparticle band structure associated to the single polaron, the energy gain induced through restoration of translational symmetry has been considered elsewhere [15]. The calculated dispersion band of a single polaron is shown in Fig. 3. Because of the antiferromagnetic background, the band has twice the lattice periodicity. Exact calculations in finite clusters do not show this periodicity, as the solutions have a well defined spin and mix different background textures. As cluster sizes are increased, however, exact solutions tend to show the extra periodicity of our results. We interpret this as a manifestation that spin invariance is broken in the thermodynamic limit, because of the antiferromagnetic background. Hence, the lack of this symmetry in our calculations should not induce spurious effects. Fig. 3 shows the polaron bandwidth as a function of U. It behaves as t^2/U, the fitted law being

$$E_{\rm BW} = -0.022t + 11.11\frac{t^2}{U} \tag{24}$$

This result indicates that the band width tends to zero as U approaches infinite, as observed in the results for the energy gain reported in [15]. Our scheme allows a straightforward explanation of this scaling. Without reversing the spin of the whole background, the polaron can only hop within a given sublattice. This implies an intermediate virtual hop into a site with an almost fully localized electron of the opposite spin. The amplitude of finding a reversed spin in this new site decays as t^2/U at large U.

On the other hand, we find that the dispersion relation can be satisfactorily fitted by the expression:

$$\epsilon_{\mathbf{k}} = \epsilon_0 + 4t_{11}\cos(k_x)\cos(k_y) + 2t_{20}[\cos(2k_x) + \cos(2k_y)] + 4t_{22}\cos(2k_x)\cos(2k_y) + 4t_{31}[\cos(3k_x)\cos(k_y) + \cos(k_x)\cos(3k_y)]. \tag{25}$$

For $U = 8t$, we get $t_{11} = 0.1899t$, $t_{20} = 0.0873t$, $t_{22} = -0.0136t$, and $t_{31} = -0.0087t$. All hopping integrals vanish as t^2/U in the large U limit for the reason given above. Also the energy gain with respect to UHF [16] behaves in this way. All these features are in good agreement with known results [3–6] for both the Hubbard and the $t - J$ models.

B. Two Holes

We now consider solutions with two spin polarons. The relevant UHF solutions are those with $S_z = 0$ (solutions with $S_z = 1$ will also be briefly considered). In order for the coupling to be finite, the centers of the two spin polarons must be located in different sublattices. The mean field energy increases as the two polarons are brought closer, although, for intermediate and large values of U, a locally stable Hartree Fock solution can be found with two polarons at arbitrary distances. We have not attempted to do a full CI analysis of all possible combinations of two holes in a finite cluster. Instead, we have chosen a given mean field solution (UHF) and hybridized it with all others obtained by all lattice translations and rotations. Some results of calculations in which more than one UHF solution is included will be also presented. Clusters of sizes up to 10×10 were studied which, as in the case of the polaron, are large enough due to the short–range interactions between different configurations. The basis used for the two polarons at the shortest distance is shown in Fig. 2. This procedure leads to a set of bands, whose number depends on the number of configurations included in the CI calculation. For instance if the basis set of Fig. 2 is used four bands are obtained (see also below).

Like in the single polaron case, we obtain a gain in energy (with respect to UHF), due to the delocalization of the pair. The numerical results for L=6, 8 and 10 and U in the range $8t - 5000t$ are shown in the inset of Fig. 4. They can be fitted by the following straight lines,

$$E_{\rm G}^{1,0} = 0.495t + 1.53\frac{t^2}{U} \tag{26a}$$

$$E_{\rm G} = -0.002t + 3.78\frac{t^2}{U} \tag{26b}$$

where (26a) corresponds to holes at the shortest distance and (26b) to holes at the largest distance. Note that, whereas in the case of the holes at the largest distance, the gain goes to zero in the large U limit, as for the isolated polaron, when the holes are separated by a $\{1, 0\}$ vector the gain goes to a finite value. This result is not surprising, as the following arguments suggest. The hopping terms in the bipolaron calculation, that are proportional to t at large U, describe the rotation of a pair around the position of one of the two holes. Each hole is spread between four sites. In order for a rotation to take place, one hole has to jump from one of these sites into one of the rotated positions. This process can always take place without a hole moving into a fully polarized site with the wrong spin. There is a gain in energy, even when $U/t \to \infty$. In the single polaron case, the motion of a hole involves the inversion of, at least, one spin, which is fully polarized in the large U limit. Because of this, hybridization gives a vanishing contribution to the energy as $U/t \to \infty$.

The results discussed above are in line with those for the width of the quasiparticle band. The numerical results can be fitted by,

$$E_{\rm BW}^{1,0} = 3.965t + 14.47\frac{t^2}{U} \tag{27a}$$

$$E_{\rm BW} = -0.007t + 10.1\frac{t^2}{U} \tag{27b}$$

Thus, the total bandwidth of the two bands obtained for holes in neighboring sites does not vanish in the infinite U limit (as the energy gain reported in Fig. 2). The internal consistency of our calculations is shown comparing the large U behavior of the two holes at the largest distance possible with the corresponding results obtained for the isolated polaron (compare this fitting with that given in Eq. (24)) .

The hole–hole interaction, i.e., the difference between the energy of a state built up by all configurations with the two holes at the shortest distance (separated by a vector of the set {1,0}) and the energy of the state having the holes at the largest distance possible at a given cluster is depicted in Fig. 4. Two holes bind for intermediate values of U [36]. This happens because the delocalization energy tends to be higher than the repulsive contribution obtained within mean field. The local character of the interactions is illustrated by the almost null dependence of the results shown in Fig. 4 on the cluster size.

The only numerical calculations which discuss the binding of holes in the Hubbard model are those reported in [8]. Energetically, it is favorable to pair electrons in a 4×4 cluster for values of U/t greater than 50. The analysis of the correlation functions suggests that pairing in real space ceases at $U/t \sim 16$, leading to the suspicion of large finite size effects. Our results give that pairing dissappears at $U/t \approx 40$, which is consistent with the analysis in [8]. Similar

calculations for the t-J model give binding between holes for $J/t \geq 0.1$ [10]. Taking $J = \frac{4t^2}{U}$, this threshold agrees well with our results.

In order to clarify some aspects of the method, we have carried out a more detailed analysis of two hole solutions in 6×6 clusters. The results are presented in Table V. Within UHF the most favorable solution is that with the two holes at the largest distance (2,3) but for the smallest U shown in the Table. The solution with the holes at the shortest distance (1,0) is only favored at small U, while for $U \geq 8$ even the solution with $S_z = 1$ has a smaller energy. Instead when the lattice symmetry is restored the solution with the holes at the shortest distance is the best for all U excluding $U = 200$. For such a large U the wavefunction constructed with all configurations from {2,3} has the lowest energy. The solution with $S_z = 1$ is unfavorable for all U shown in Table V, in contrast with the results found in the 4×4 cluster, indicating that size effects were determinant in the results for the smaller cluster. Including all configurations with S_z either 1 or 0 does not change this trend. The small difference between the results for {1,0} and those with all configurations with $S_z = 0$ for large U is misleading. In fact, the weight of the configuration with the holes at the largest distance (2,3) in the final CI wavefunction increases with U. This will be apparent in the hole–hole correlations discussed in the following paragraph.

We have analysed the symmetry of the ground state wavefunction $|\Psi\rangle$ obtained with all configurations having the holes at the shortest distance. The numerical results for all U show that $\langle\Phi^1|\Psi\rangle = -\langle\Phi^2|\Psi\rangle = \langle\Phi^3|\Psi\rangle = -\langle\Phi^4|\Psi\rangle$, where the $|\Phi^i\rangle$ are the four configurations shown in Fig. 2. This symmetry corresponds to the $d_{x^2-y^2}$ symmetry, in agreement with previous theoretical studies of the Hubbard and $t--J$ models [37,38].

The quasiparticle band structure for two holes has also been investigated. The main interactions t_i and the overlaps s_i between the configurations are given in Table VI (the meaning of the symbols is specified in Fig. 2). The results correspond to a 6×6 cluster with the two holes at the shortest distance. At finite U many interactions contribute to the band, in Table VI we only show the largest ones. Of particular significance is the t_3 interactions which accounts for the simultaneous hopping of the two holes. This term, which clearly favors pairing, vanishes in the infinite U limit, in line with the results for the hole–hole interaction (see above) which indicate that pairing is not favored at large U. Also in this limit $t_1 = t_2$. Including only the interactions given in Table VI, the bands can be easily obtained from,

$$\begin{vmatrix} E + 2(s_1E - t_1)\cos k_x + 2(s_3E - t_3)\cos k_y & (s_2E - t_2)(1 + \mathrm{e}^{\mathrm{i}k_x})(1 + \mathrm{e}^{-\mathrm{i}k_y}) \\ (s_2E - t_2)(1 + \mathrm{e}^{-\mathrm{i}k_x})(1 + \mathrm{e}^{\mathrm{i}k_y}) & E + 2(s_1E - t_1)\cos k_y + 2(s_3E - t_3)\cos k_x \end{vmatrix} = 0 \tag{28}$$

Neglecting the overlap, the bands are given by,

$$E(\mathbf{k}) = (t_1 + t_3)(\cos k_x + \cos k_y) \pm \sqrt{[(t_1 + t_3)(\cos k_x + \cos k_y)]^2 + 4t_2^2(1 + \cos k_x)(1 + \cos k_y)} \tag{29}$$

In the infinite U limit ($t_3 = 0$ and $|t_1| = |t_2|$) the bands are simply,

$$E_1(\mathbf{k}) = -2t_1 \tag{30a}$$

$$E_2(\mathbf{k}) = 2t_1(1 + \cos k_x + \cos k_y) \tag{30b}$$

Note that, as in the single hole case and due to the antiferromagnetic background, the bands have twice the lattice periodicity. The dispersionless band has also been reported in [34] and, in our case, it is a consequence of the absence of two hole hopping in the infinite U limit ($t_3 = 0$). Our results, however, disagree with the conclusions reached in [34] concerning the absence of hole attraction. We find a finite attraction for holes at intermediate U's. It is interesting to note that our effective hopping is of order t, and not of order t^2/U as in citeCK98. This effect is due to the delocalized nature of the single polaron texture (5 sites, at least), and it does not correspond to a formally similar term which can be derived from the mapping from the Hubbard to the t-J model [39].

The results for the hole–hole correlation, $\langle(1 - n_i)(1 - n_j)\rangle$, as function of the hole–hole distance $r_{ij} = |\mathbf{r}_i - \mathbf{r}_j|$ are reported in Tables VII and VIII. The normalization $\sum_j \langle(1-n_i)(1-n_j)\rangle = 1$ has been used. The results correspond to CI wavefunctions with $S_z = 0$ and were obtained including all configurations from either the set {1,0} or from the sets {1,0}, {1,2}, {3,0} and {2,3}. The results are in qualitative agreement with those in [8]. When comparing with results obtained for the t-J model, one must take into account that, in the Hubbard model, the hole–hole correlation, as defined above, can take negative values (see Appendix). This is due to the appearance of configurations with double occupied sites, which are counted as negative holes. Aside from this effect, our results describe well a somewhat puzzling result found in the t-J model (see for instance [13,29,40]): the maximum hole–hole correlation occurs when the two holes are in the same sublattice, at a distance equal to $\sqrt{2}$ times the lattice spacingi [41]. This result follows directly from the delocalized nature of the spin polarons, as seen in Fig. 1. The center of each spin polaron propagates through one sublattice only, but the electron cloud has a finite weight in the other one, even when $U/t \to \infty$. This

effect is noted in all cases but for $U = 200$ with all configurations. In that case there is not a clear maximum and the correlations are appreciable even at rather large distances. The reason for this behavior is that for large U the configuration with the holes at the largest distance, namely, {2,3}, have the lowest energy and, thus, a large weight in the CI wavefunction. This is consistent with the fact that no attraction was observed at large U (see Fig. 4). Finally we note that the slower decrease with distance of hole–hole correlations, obtained for $U = 8$ including configurations from the four sets (Table VIII) may be a consequence of the decrease in the difference between UHF and CI energies as U diminishes (see Fig. 4).

C. Four Holes

An interesting question is whether the holes would tend to segregate when more holes are added to the cluster. In order to investigate this point, we have calculated total energies for four holes on 10×10 clusters with the holes either centered on a square, or located on two bipolarons separated by a (5,5) vector and with the holes at the shortest distance. Two (four) configurations (plus translations) were included in each case. In the case of two bipolarons only configurations in which the two bipolarons are rotated simultaneously are included. Other possible configurations have different energies and contribute to a less extent to the wavefunction. In any case, increasing the size of the basis set would not have changed the essential conclusion of our analysis (see below). The results for several values of U are shown in Table IX. We note that already at the UHF level the solution with two separated bipolarons has a lower energy. The Coulomb repulsion term in the Hamiltonian does not favor the configuration with the aggregated holes but for very small U. Restoring lattice symmetry decreases the energy in both cases to an amount which in neither case vanishes in the infinite U limit. The decrease is slightly larger in the case of the four holes on a square. This result can be understood by noting that the holes move more freely (producing the smallest distortion to the AF background) when the charge is confined to the smallest region possible. In any case, this is not enough to compensate the rather important difference in energy between the two cases at the UHF level. These results indicate that for large and intermediate U no hole segregation takes place and that the most likely configuration is that of separated bipolarons.

D. Effective Hamiltonian for Hole Pairing

As discussed above, in the large U limit the bipolaron moves over the whole cluster due to the interactions among the four mean field wavefunctions of Fig. 2 (interactions t_1 and t_2 in Fig. 5). This mechanism can be viewed as another manifestation of hole assisted hopping. The possibility of hole assisted hopping has been already considered in [42], although in a different context. It always leads to superconductivity. In our case, we find a contribution, in the large U limit, of the type:

$$\mathcal{H}_{hop} = \sum \Delta t {c^\dagger}_{i,j;s} c_{i,j;s} ({c^\dagger}_{i+1,j;\bar{s}} c_{i,j+1;\bar{s}} + \\ + {c^\dagger}_{i-1,j;\bar{s}} c_{i+1,j;\bar{s}} + h.c. + \text{perm}) \tag{31}$$

This term admits the BCS decoupling $\Delta t \langle c^\dagger_{i,j;s} c^\dagger_{i+1,j;\bar{s}} \rangle c_{i,j;s} c_{i,j+1;\bar{s}} + h.c. + ...$ It favors superconductivity with either s or d wave symmetry, depending on the sign of Δt. Since we find $\Delta t > 0$, d–wave symmetry follows.

VI. CONCLUDING REMARKS

We have analyzed the leading corrections to the Hartree Fock solution of the Hubbard model, with zero, one and two holes. We show that a mean field approach gives a reasonable picture of the undoped system for the entire range of values of U/t.

The main drawback of mean field solutions in doped systems is their lack of translational invariance. We overcome this problem by using the Configuration Interaction method. In the case of one hole, the localized spin polaron is replaced by delocalized wavefunctions with a well defined dispersion relation. The bandwidth, in the large U limit, scales as $\frac{t^2}{U}$, and the solutions correspond to spin polarons delocalized in a given sublattice only. As in the undoped case, these results are in good agreement with other numerical calculations, for the Hubbard and t-J models.

The same approach is used to analyze the interactions between pairs of holes. We first obtain Hartree Fock solutions with two holes at different separations. From comparing their respective energies, and also with single

hole solutions, we find a short range repulsive interaction between holes. This picture is significantly changed when building delocalized solutions. The energy gain from the delocalization is enough to compensate the static, mean field, repulsion. There is a net attractive interaction for $8 \leq U/t \leq 50$, approximately. The correlations between the holes which form this bound state are in good agreement with exact calculations, when available. The state has $d_{x^2-y^2}$ symmetry. In this range of parameters, we find no evidence of hole clustering into larger structures.

A further proof of the efficiency ot the present CI approach results from a comparison with the CI approach of [28], that is based upon an extended basis (**k**–space). For a 6×6 cluster and $U = 4$ the UHF localized solution has an energy of -31.747. A CI calculation including 36 localized configurations lowers the energy down to -31.972. This has to be compared with the result reported in [28] obtained by means of 2027860 extended configurations, namely, -30.471. The difference between the two approaches should further increase for larger U.

We have not applied the same technique to other Hartree Fock solutions which have been found extensively in the Hubbard model: domain walls separating antiferromagnetic regions [20,44–46]. The breakdown of translational symmetry associated with these solutions is probably real and not just an artifact of the Hartree Fock solution, as in the previous cases. Hybridization of equivalent solutions can, however, stabilize domain walls with a finite filling, which are not the mean field solutions with the lowest energy.

Because of the qualitative differences between spin polarons and domain walls, we expect a sharp transition between the two at low values of U/t. Note, however, that the scheme presented here, based on mean field solutions plus corrections, is equally valid in both cases.

ACKNOWLEDGMENTS

Financial support from the CICYT, Spain, through grants PB96-0875, PB96-0085, PB95-0069, is gratefully acknowledged.

VII. APPENDIX: HOLE-HOLE CORRELATIONS IN THE HYDROGEN MOLECULE

Here we explicitly calculate the hole–hole correlations in the hydrogen molecule described by means of the Hubbard model. Let us call $a^\dagger_\sigma$ and $b^\dagger_\sigma$ the operators that create a particle with spin σ at sites a and b respectively. The ground state wavefunction has $S_z = 0$ and is given by,

$$|\psi> = (2+\alpha^2)^{-1/2} \left(|\phi_1> + |\phi_2> + |\phi_3>\right) \tag{32}$$

where,

$$|\phi_1> = a^\dagger_\uparrow b^\dagger_\downarrow |0> \tag{33a}$$

$$|\phi_2> = \frac{1}{\sqrt{2}} \left(a^\dagger_\uparrow a^\dagger_\downarrow + b^\dagger_\uparrow b^\dagger_\downarrow\right) |0> \tag{33b}$$

$$|\phi_3> = b^\dagger_\uparrow a^\dagger_\downarrow |0> \tag{33c}$$

with

$$\alpha = \frac{E}{\sqrt{2}}, \quad E = \frac{U}{2} - \left(\frac{U^2}{4} + 4\right)^{1/2} \tag{34}$$

The wavefunctions in Eq. (33) are orthonormalized, namely, $<\phi_i|\phi_j> = \delta_{ij}$. The result for the hole–hole correlations on different sites is,

$$<\psi|(1-n_a)(1-n_b)|\psi> = -\frac{\alpha^2}{2+\alpha^2} \tag{35}$$

As $\alpha = -\sqrt{2}, 0$ when $U = 0, \infty$, this expectation value varies from -0.5 to 0.0. Thus it can take negative values as found in the case of clusters of the square lattice. Instead, the hole–hole correlation on the same site is given by,

$$< \psi|(1-n_a)(1-n_a)|\psi >= \frac{\alpha^2}{2+\alpha^2} \tag{36}$$

which is positive for all values of U. Particle–particle correlations are obtained by adding 1 to these results.

---

[1] A.P. Kampf, Phys. Rep.. **249**, 219 (1994).
[2] D.J. Scalapino, Phys. Rep. **250**, 329 (1995).
[3] N. Bulut, D. J. Scalapino and S. R. White, Phys. Rev. Lett. **72**, 705 (1994).
[4] R. Preuss, W. van der Linden and W. Hanke, Phys. Rev. Lett. **75**, 1344 (1995).
[5] E. Dagotto, A. Nazarenko and M. Boninsegni, Phys. Rev. Lett. **73**, 728 (1994).
[6] P. W. Leung and R. J. Gooding, Phys. Rev. B **52**, R15711 (1995).
[7] D. Duffy, A. Nazarenko, S. Haas, A. Moreo, J. Riera and E. Dagotto, Phys. Rev. B **56**, 5597 (1997).
[8] G. Fano, F. Ortolani and A. Parola, Phys. Rev. B **42**, 6877 (1990)
[9] M. Boninsegni and E. Manousakis, Phys. Rev. B **47**, 11897 (1993).
[10] D. Poilblanc, J. Riera and E. Dagotto, Phys. Rev. B **49**, 12318 (1994).
[11] E. Dagotto, Rev. Mod. Phys. **66**, 763 (1994).
[12] K. Kuroki and H. Aoki, preprint, `cond-mat/9710019`.
[13] C. Gazza, G. B. Martins, J. Riera and E. Dagotto, preprint `cond-mat/9803314`).
[14] S. Zhang, J. Carlson and J. E. Gubernatis, Phys. Rev. Lett. **78**, 4486 (1997).
[15] E. Louis, G. Chiappe, J. Galán, F. Guinea and J. A. Vergés, Phys. Rev. B **48**, 426 (1993).
[16] E. Louis, G. Chiappe, F. Guinea, J. A. Vergés and E. V. Anda, Phys. Rev. B **48**, 9581 (1993).
[17] E. Louis, F. Guinea, M.P. López–Sancho and J.A. Vergés, Europhys. Lett., **44**, 229 (1998).
[18] G. Seibold, E. Sigmund and V. Hizhnykov, Phys. Rev. B **57**, 6937 (1998).
[19] G. Seibold, Phys. Rev. B, in press (cond-mat/9809113).
[20] J. A. Vergés, E. Louis, P.S. Lomdahl, F. Guinea and A. R. Bishop, Phys. Rev. B **43**, 6099 (1991).
[21] F. Guinea, E. Louis and J. A. Vergés, Phys. Rev. B **45**, 4752 (1992).
[22] J. E. Hirsch, Phys. Rev. Lett. **59**, 228 (1987).
[23] A. Kampf and J. R. Schrieffer, Phys. Rev. B **41**, 6399 (1990).
[24] E. Dagotto and J. R. Schrieffer, Phys. Rev. B **43**, 8705 (1990).
[25] A. Auerbach, *Interacting electrons and quantum magnetism*, Springer Verlag, New York (1994).
[26] E. Louis, J. Galán, F. Guinea, J. A. Vergés and J. Ferrer, Phys. Sta. Sol. (b) **173**, 715 (1992).
[27] A. Ramsak and P. Horsch, Phys. Rev. B **57**, 4308 (1998).
[28] B. Friedman and G. Levine, Phys. Rev. B **55**, 9558 (1997).
[29] S. R. White and D. J. Scalapino, Phys. Rev. B **55**, 6504 (1997).
[30] R. B. Laughlin *A Critique of Two Metals*, preprint `cond-mat/9709195` (1997).
[31] P. W. Anderson and G. Baskaran, *A Critique of "A Critique of Two Metals "*, preprint `cond-mat/9711197` (1997).
[32] R. Chitra and G. Kotliar, *Dynamical Mean Field Theory of the Antiferromagnetic Metal to Antiferromagnetic Insulator Transition*, preprint `cond-mat/9811144` (1998).
[33] E. Dagotto and T. M. Rice, Science **271**, 618 (1996).
[34] E. W. Carlson, S. A. Kivelson, Z. Nussinov and V. J. Emery, Phys. Rev. B **57**, 14704 (1998).
[35] A. W. Sandvik, Phys. Rev. B **56**, 11678 (1997).
[36] Note that at large U the ferromagnetic solution sets in. In Ref. [15] it was shown that the energy of two holes in a ferromagnetic $L \times L$ cluster could be fitted by $E/t = -7.942 + 31.02/L^2$. Comparing the present numerical results with this energy gives a transition to the ferromagnetic solution approximately at $U/t = 32$, for the cluster sizes investigated here.
[37] E. Dagotto, Rev. Mod. Phys. **66**, 763 (1994).
[38] M. Cyrot and D. Pavuna, *Introduction to Superconductivity and High–T_c Materials*, World Scientific (1992).
[39] S. Trugman, Phys. Rev. B **37**, 1597 (1988).
[40] J. Riera and E. Dagotto, Phsy. Rev. B **57**, 8609 (1997).
[41] Note that this results is obtained whithout including configurations which clearly favor it, such as that proposed in [40] in which the two holes lie on neighboring sites along a diagonal and a neighboring spin is flipped.
[42] J. E. Hirsch, Phys. Rev. B **48**, 3327 (1993).
[43] A. V. Dotsenko, Phys. Rev. B **57**, 6917 (1998).
[44] J. Zaanen and O. Gunnarsson, Phys. Rev. B **40**, 7391 (1989).
[45] D. Poilblanc and T. M. Rice, Phys. Rev. B **39**, 9749 (1989).
[46] H. J. Schulz, Phys. Rev. Lett. **64**, 1445 (1990).

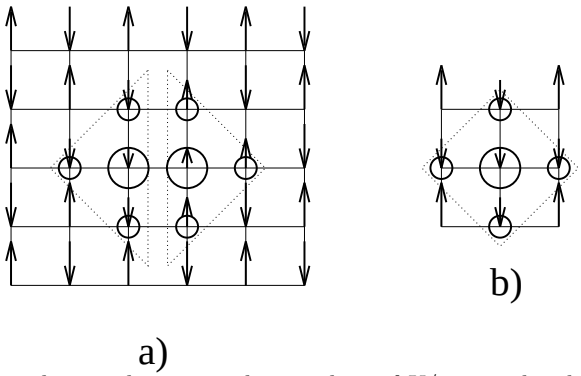

FIG. 1. a) Sketch of one of the bipolaron solutions, at large values of U/t, considered in the text. Circles denote the local charge, measured from half filling, and arrows denote the spins. There are two localized states marked by the dashed line. For comparison, the single polaron solution is shown in b).

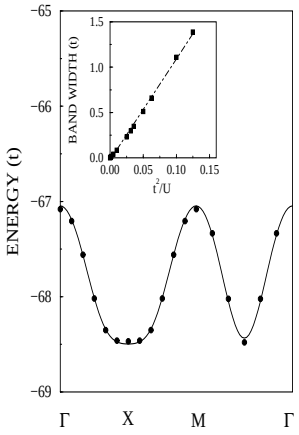

FIG. 2. Sketch of the bipolaron UHF wavefunctions used in this work. Note that the four wavefunctions are obtained by successive rotations of $\pi/2$. The complete basis set is produced by translation of these wavefunctions through the whole cluster.

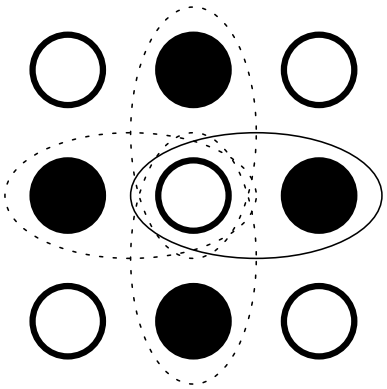

FIG. 3. Quasiparticle band structure for a single hole on 12×12 clusters of the square lattice with periodic boundary conditions and $U = 8$. The continuous line corresponds to the fitted dispersion relation (see text). The inset shows the bandwidth as a function of t^2/U for $U \geq 8t$; the fitted straight line is $-0.022t + 11.11t^2/U$.

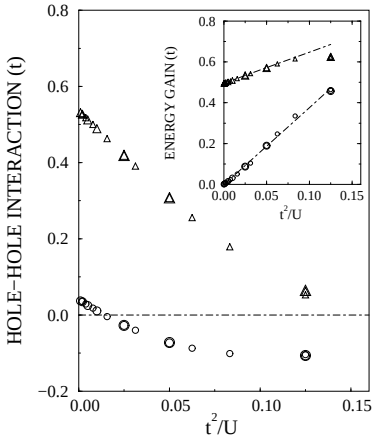

FIG. 4. Comparison of the hole–hole interaction (see main text for the definition) obtained within UHF (triangles) and CI (circles) approximations for wavefunctions with $S_z = 0$. Results correspond to 6×6, 8×8 and 10×10 clusters with periodic boundary conditions, and $U \geq 8t$. The size of the symbols increases with increasing cluster size. The inset shows the energy gain due to the inclusion of correlation effects via CI for both the configuration of holes located in neighboring positions (circles) and holes that are maximally separated in the finite size cluster (triangles). The respective asymptotic behaviors for large U are: $0.495t + 1.53t^2/U$ for holes at the shortest distance and $-0.002t + 3.78t^2/U$ for holes at the largest distance.

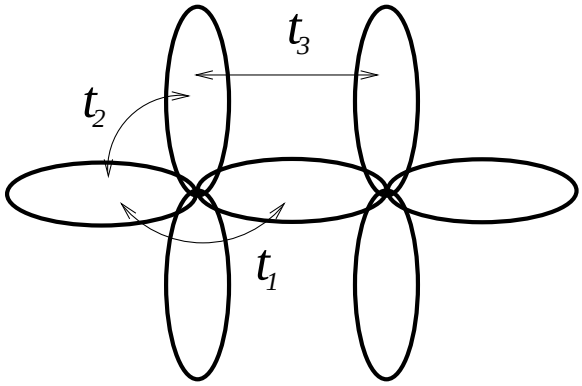

FIG. 5. Interactions between two hole configurations having the holes at the shortest distance (separated by a (1,0) vector).

TABLE I. Exact [8], UHF and CI (see text) energies of the Hubbard model versus U, for the half–filled 4×4 cluster. All energies are given in units of the hopping integral t. The UHF solution of lowest energy corresponds to the antiferromagnetic (AF) configuration while the CI results were obtained by adding to the AF configuration the 32 configurations having two neigboring spins flipped (referred to as sf). The interaction and overlap between the AF and the sf configurations ($S_{\mathrm{AF,sf}}$ and $t_{\mathrm{AF,sf}}$) are also given.

	Exact	UHF		CI		
U	Exact	AF	sf	AF+sf	$t_{\mathrm{AF,sf}}$	$S_{\mathrm{AF,sf}}$
6	-10.55222	-9.37989	-7.94663	-9.85296	1.1410	0.1035
8	-8.46887	-7.38963	-6.16154	-7.87777	0.5863	0.0572
16	-4.61186	-3.91165	-3.20231	-4.27171	0.1692	0.0150
32	-2.37589	-1.98846	-1.61884	-2.19194	0.0682	0.0039
50	-1.53078	-1.27695	-1.03838	-1.41060	0.0415	0.0016
100	-	-0.63962	-0.51980	-0.70736	0.0202	0.0004

TABLE II. UHF and CI (see text) energies of the Hubbard model in the 4×4 cluster for several values of U and 1 and 2 holes (with respect to half–filling). All energies are given in units of the hopping integral t. The CI results for 2 holes were obtained by including all configurations having the holes separated by vectors of the sets {1,0} or {2,1}. The CI calculation for 1 hole includes the spin polaron configuration. In both cases the full basis set was constructed by restoring point and translational symmetries.

	1		2			
U	UHF	CI	UHF-(1,0)	CI-{1,0}	UHF-(2,1)	CI-{2,1}
4	-13.30222	-13.36021	-14.09307	-14.20511	-14.09240	-14.16640
6	-10.27549	-10.59418	-11.18149	-11.65669	-11.12471	-11.55214
8	-8.46151	-8.76271	-9.47288	-9.94496	-9.47043	-9.81703
16	-5.37431	-5.53656	-6.59120	-7.08701	-6.79804	-6.97274
32	-3.70563	-3.78024	-5.04100	-5.54390	-5.40559	-5.48360
50	-3.09365	-3.13879	-4.47406	-4.97558	-4.90015	-4.94714

TABLE III. Exact and UHF or CI (see text) energies of the Hubbard model in the 4×4 cluster for several values of U 1 or 2 holes (with respect to half–filling). All energies are given in units of the hopping integral t. The CI results for 2 holes were obtained by including all {1,0} and {2,1} configurations (see also caption of Table II).

	Exact		CI	
U	1	2	1	2
4	-14.66524	-15.74459	-13.36021	-14.48135
6	-11.96700	-13.42123	-10.59418	-11.81262
8	-10.14724	-11.86883	-8.76271	-10.17505
16	-6.80729	-9.06557	-5.53656	-7.21100
32	-4.93556	-7.56832	-3.78024	-5.59560
50	-4.25663	-7.07718	-3.13879	-5.00862

TABLE IV. Same as Table II for two holes wavefunctions with $S_z = 1$. The energy of the CI solution corresponding to (2,2) almost coincides with that of its UHF solution. Including all configurations of the sets {1,1} and {2,2}, does not change the result obtained with only the former set.

	UHF		CI
U	(1,1)	(2,2)	{1,1}
6	-11.12980	-10.89495	-11.77834
8	-9.48701	-9.37275	-10.11391
16	-6.77454	-6.78954	-7.10740
32	-5.33285	-5.41009	-5.48456
50	-4.80587	-4.90506	-4.89772

TABLE V. UHF and CI (see text) energies of the Hubbard model in the 6 × 6 cluster for two holes (with respect to half–filling) and several values of U. All energies are given in units of the hopping integral t. The UHF results correspond to the configurations with the two holes at the shortest distance with either $S_z = 0$ or 1 separated by lattice vectors (1,0) or (1,1), respectively, and at the largest distance with $S_z = 0$ -holes separated by a (2,3) vector. The CI results were obtained by including all configurations derived either from the sets {1,0} or {2,3} (a total of 72 configurations), the set {1,1} (36 configurations) all sets having $S_z = 0$, namely, {1,0}, {2,1}, {3,0} and {2,3} (324 configurations) or all sets having $S_z = 1$, i.e., {1,1}, {2,2}, {3,1} and {3,3} (117 configurations).

	UHF			CI				
U	(1,0)	(2,3)	(1,1)	{1,0}	{2,3}	{1,1}	all $S_z = 0$	all $S_z = 1$
6	-23.147	-23.121	-23.063	-23.704	-23.608	-23.352	-23.813	-23.700
8	-18.867	-18.920	-18.848	-19.488	-19.385	-19.075	-19.586	-19.448
20	-9.952	-10.260	-10.159	-10.525	-10.452	-10.285	-10.562	-10.479
200	-4.120	-4.632	-4.500	-4.622	-4.647	-4.510	-4.652	-4.650

TABLE VI. Absolute value of the interactions t_i and overlaps s_i between the configurations included in the case of two holes at the shortest distance, for several values of the interaction parameter U. The meaning of the symbols is given in Fig. 5. The results correspond to the 6 × 6 cluster.

U	t_1	t_2	t_3	s_1	s_2	s_3
8	2.459	4.672	1.202	0.124	0.235	0.056
20	1.418	1.624	0.159	0.119	0.135	0.009
200	0.646	0.651	0.007	0.088	0.088	9×10^{-5}
2000	0.584	0.584	7×10^{-4}	0.084	0.084	9×10^{-7}

TABLE VII. Hole–hole correlations $\langle(1-n_i)(1-n_j)\rangle$ as a function of the hole–hole distance r_{ij} for three values of U. The results correspond to two holes in 6 × 6 clusters and were obtained including all configurations of the set {1,0}. The normalization $\sum_j\langle(1-n_i)(1-n_j)\rangle = 1$ was used.

r_{ij} / U	8	20	200
0	1.4	0.657	0.491
1	-0.171	-2.51×10^{-3}	3.27×10^{-2}
$\sqrt{2}$	3.99×10^{-2}	6.30×10^{-2}	6.97×10^{-2}
2	2.0×10^{-3}	1.43×10^{-3}	3.97×10^{-4}
$\sqrt{5}$	9.6×10^{-3}	9.55×10^{-3}	9.54×10^{-3}
$2\sqrt{2}$	3.34×10^{-3}	8.43×10^{-4}	7.53×10^{-4}
3	4.54×10^{-3}	4.18×10^{-3}	6.03×10^{-3}
$\sqrt{10}$	2.46×10^{-3}	6.66×10^{-4}	7.53×10^{-4}
$\sqrt{13}$	1.49×10^{-3}	8.51×10^{-4}	7.53×10^{-4}

TABLE VIII. As in Table VII, but including all configurations from the sets {1,0}, {2,1}, {3,0} and {2,3}.

r_{ij} / U	8	20	200
0	1.367	0.664	0.493
1	-0.183	-1.08×10^{-2}	5.18×10^{-3}
$\sqrt{2}$	2.38×10^{-2}	5.18×10^{-2}	7.65×10^{-3}
2	4.37×10^{-3}	3.06×10^{-3}	2.36×10^{-2}
$\sqrt{5}$	8.57×10^{-3}	8.99×10^{-3}	1.59×10^{-2}
$2\sqrt{2}$	9.48×10^{-3}	5.20×10^{-3}	7.48×10^{-3}
3	1.30×10^{-2}	7.47×10^{-3}	4.43×10^{-2}
$\sqrt{10}$	8.86×10^{-3}	4.64×10^{-3}	2.36×10^{-2}
$\sqrt{13}$	1.74×10^{-2}	6.4×10^{-3}	5.06×10^{-3}

TABLE IX. UHF and CI energies (in units of the hopping integral t) for 4 holes in 10×10 clusters and several values of the interaction U. The results correspond to configurations with either the four holes on a square (denominated as 4) or on two bipolarons (2+2) separated by a (5,5) vector.

	4		2+2	
U	UHF	CI	UHF	CI
8	-50.500	-50.828	-50.782	-51.242
16	-29.208	-29.629	-29.922	-30.321
32	-17.588	-17.989	-18.574	-18.921
128	-8.651	-9.005	-9.851	-10.148
512	-6.406	-6.744	-7.659	-7.941
4096	-5.750	-6.084	-7.020	-7.297